Energy-Efficient Massive MIMO With Decentralized Precoder Design

Shuai Zhang , *Student Member, IEEE*, Bo Yin , *Member, IEEE*, Yu Cheng , *Senior Member, IEEE*,
Lin X. Cai , *Senior Member, IEEE*, Sheng Zhou , *Member, IEEE*, Zhisheng Niu , *Fellow, IEEE*,
and Hangguan Shan , *Member, IEEE*

Abstract—This paper presents an energy-efficient downlink pre-coding scheme in a multi-cell Massive MIMO system. We approach the precoder design problem to maximize the system energy efficiency by jointly considering power control, interference management, antenna switching and user throughput in a cluster of base stations. This is computationally difficult as it requires solving a sparsity-inducing non-convex optimization problem, which is NP-hard. To alleviate the solution complexity, first a stochastic smooth approximation of zero-norm is applied in the antenna power management to enable fast, gradient-based algorithms. For efficient convergence, we develop a novel optimization algorithm combining augmented multiplier (AM) and quadratic programming (QP), and show how this scheme permits decentralized implementation by offloading parts of the computation to the individual base stations to reduce communication overhead. We provide theoretical proof that the proposed algorithm converges both locally and globally under realistic assumptions. Numerical results confirm that our method achieves higher energy efficiency with a superior convergence rate compared to different types of existing methods, and illustrate the relationship between energy efficiency performance and system design parameters.

Index Terms—Massive MIMO, 5G, beamforming, energy-efficiency, distributed optimization.

I. INTRODUCTION

THE central theme in developing the next generation mobile communication system is the drive for higher data rate at lower energy consumption. Today's communication system

designer must be aware of both the throughput performance as well as the corresponding power cost, and as a result Energy Efficiency (EE) has become an important metric for network evaluation and optimization [1]–[3]. EE is defined as the ratio of the achieved throughput (in bits/s) to the corresponding power consumption in Watts. It is a direct measurement of how efficiently the system transports bits of information, and can be used as a guideline for system optimization.

To push the boundaries of a high-EE operating regime, massive MIMO is a technology under active development for 5G New Radio [4], the radio access standardization for the fifth-generation mobile networks. Its feature is by using an excessive number of base station (BS) antennas, typically an order of magnitude higher than the number of served users, to achieve an aggressive diversity gain. This is made possible by two beneficial properties, *favorable propagation* and *channel hardening*: as the number of BS antennas increases, the channels of different users become increasingly close to its expectation and orthogonal to each other [5]. Consequently, adverse effects like fading, intra-cell interference and uncorrelated noise can be mitigated with simple signal processing techniques like linear *precoding*, i.e., constructing the signal on each transmit antenna as a weighted combination of the signals for different data streams, when there are sufficiently many antennas. According to the theoretical analysis [5], a system with M antennas and K users ($M \gg K$) could achieve $O(M)$ gain in effective signal-to-noise-ratio (SNR), indicating achievable equal throughput with only $1/M$ power consumption compared to the single-antenna system.

On the other hand, this kind of configuration necessarily requires the deployment of a large number of antennas and the corresponding radio circuits, which is considered to be inefficient energy-wise and could affect the practicality of deploying massive MIMO systems. This issue has spurred a large body of research work to improve the system energy-efficiency despite using many antennas [6].

There are proposals to use a *hybrid precoding* scheme consisting of both digital and analog precoders to reduce the number of transceiver chains needed [7]. The signal is first passed through a digital precoder where its phase and amplitude are adjusted, and then analog phase shifters, which can be shared by more than one data streams, are applied to provide the additional changes in phases; because the number of data streams after digital processing can be smaller than the number of transmit

antennas, less full-scale transceiver chains are needed, and phase shifters naturally integrate into the following RF up-conversion with little additional overhead, thus saving hardware cost and less operation power. The drawback is that hybrid schemes suffer from a low degree-of-freedom, limiting the potential diversity gain from using massive MIMO. Moreover, the interference between users, introduced through either sharing or hardware imperfections, is non-negligible and deteriorates system performance. In this paper we do not consider a hybrid scheme due to these concerns, and there is evidence to suggest that the concern for transceiver chain cost may be exaggerated, as demonstrated by a recent implementation of a massive MIMO platform with 100 digital transceiver chains built with ordinary equipment [8], since each antenna element in the massive array can have relaxed requirements.

There are also works from the signal processing aspect of the problem. Since in today's communication systems there are increasingly more interacting subsystems, it is not immediately obvious whether previously proposed signal processing schemes, aiming to achieve either high system throughput or low power, can still work under high EE requirements. With the recent addition of machine learning techniques as reported [9], [10], it is still common to follow the network utility optimization path: how to maximize EE when the scenario is constrained by quality-of-service (QoS) requirements and power limits, or maintaining a certain level of fairness among users and base stations (BSs) as reported in [11]–[13].

The gain in EE would even be greater if Massive MIMO is combined with small cell deployment or network densification techniques [14]. Facing the pressure of denser deployment to satisfy the 5G network capacity demands, small cells is seen as a feasible solution. As shown by information theoretical analysis [15], smaller cell size and higher BS antenna count can both contribute to higher throughput. A typical example of it is Heterogeneous Networks (HetNet): a central master base station (MBS) provides coverage for a *macro cell*, and within it many small base stations (SBSs) form their own *small cells* as an underlay. Such an architecture is especially useful in densely populated urban areas, where a large part of the traffic comes from confined areas with high traffic called *hotspots*. A central BS may not be able to provide satisfactory QoS in an energy-efficient manner, due to either congestion, interference or unfavorable channels. In this case, small cells not only offload part of the traffic, but also reduce the power requirements for MBS because of geometrical proximity to the users. In order to take full advantage of such a heterogeneous setup for high QoS provisioning or energy efficiency, it is important to coordinate the BSs and optimize the resource allocation in HetNets [16]–[18]. For example, when the SBSs make use of the same frequency resource, the inter-tier interference can be significant; due to their small sizes users in small cells are more likely to suffer from inter-cell interference (ICI) [19], [20].

Based on these points, we study the digital precoder design problem maximizing the EE, in the scenario of a cooperating Massive MIMO-enabled small cell BS cluster. We propose a framework which jointly considers factors including power control, BS antenna switching and interference, conventionally solved as separate problems. Towards this end we show that an efficient and distributed algorithm can be applied to solve the problem.

The main contributions of this paper can be summarized as follows:

1) We consider the downlink transmission of multiple massive MIMO BSs, particularly the SBSs in a cooperative cluster. They jointly determine their power control, precoding vectors and BS antenna switching to achieve high system EE. We show that it is a general sparsity-inducing non-convex problem with a separable structure, which is considered an NP-hard problem to solve for a global solution.

2) We leverage the separable structure to transform the problem so that it can be solved in a decentralized manner. We show the series of transformations needed to arrive at the iterative algorithm combining features from Newton's method and the augmented multiplier method. We prove that the proposed method is convergent when the initial solution is sufficiently close to the optimal point, and then give additional steps to guarantee convergence no matter where the initial point is.

3) We present numerical results to demonstrate the effectiveness of the proposed algorithm, both in terms of convergence speed and achieved energy efficiencies, under different system parameters, with results from other schemes for comparison. Some useful conclusions for system deployment can be learned from the results.

Organization and Notation: The remainder of the paper is organized as follows. Section II introduces the more current state of this area of research. Section III states the system model and problem formulation. In Section IV the motivation, derivation and analysis and the transformation of the problem needed are given. Section VI presents the numerical results for performance evaluation and comparison with other methods. Section VII concludes the work and gives additional remarks. Mathematical notation note: in this paper we use calligraphic letters ($\mathcal{A}$) for sets, capital letters (A) for the set cardinality and corresponding lower-case letter as a specific member of the set ($a \in \mathcal{A}$). Bold letters denote a vector or matrix, and brackets with subscript means a set formed by enumeration, e.g. $\{x_b\}_{b \in \mathcal{B}}$ is a set of all x_b when b ranges from the set $\mathcal{B}$. $\circ$ denotes element-wise product.

II. RELATED WORK

The precoding process refers to the scaling and phase changing manipulation of transmitting signals such that the received signals could have desired properties. Massive MIMO is a natural extension of the Multi-User MIMO, where the massive number of antennas can only be put to use when precoding vectors are properly selected for a system design goal. The original paper [5] gives a closed-form expression to the key system performance metric and discusses the choice of key system parameters like the antenna and user number. Based on those, there have been many works on the design guidelines to optimize system performance metrics [21], [22]. However,

those results assume certain kinds of precoding schemes and the problem of designing an energy-efficient system when precoding scheme is also considered has yet to receive enough attention. The mainstream approach is linear precoding, which calculates the coefficients for linear combination at the receiver, for example zero-forcing, and signal-to-leakage-and-noise-ratio (SLNR). They are cheap to implement at the cost of sub-optimal system throughput. One thread of research is to extend these results to multi-cell scenarios and distribute the computation; however many do not consider the energy implications and could be operating in the low EE regime. Also a central controller which is assumed to have channel-state information from the BSs could bring high communication and processing overhead which could result in hidden energy costs; another related, but a different approach is to maximize the minimum SINR with power constraints. While easier to solve, these problems often share the drawbacks of not adapting to the current traffic: the constraints need to be reset and found by hand or another process in order to operate efficiently.

For advanced convex optimization techniques in the multi-agent setting, currently the most popular method is the Alternating Direction Multiplier Method (ADMM). In [23] ADMM is used in combination with semidefinite Relaxation to solve the coordinated beamforming with uncertainties modeled as ellipsoids in the CSI for throughput gain. The authors of [24] further extend the work to consider a general form of CSI uncertainties that gives closed-form solutions in the strongly convex cases. However they invariably need to rely on the usage of Semidefinite relaxation, which ignores one of the matrix rank constraints in order to readily apply ADMM. A joint solution regarding BS clustering and beamforming is given in [25]. [26] provides a general framework for using the primal-dual perturbation method, which can be seen as a version of the multiplier methods for optimization that has involved and coupled constraints. Another good introduction of the ADMM algorithm use in wireless networks is presented in [27], which gives the result of how to obtain an infeasibility certificate and speed-up tricks. Yet they all have to either model the problem in the convex form, which is limiting for EE design goal, or use convex approximation at local iterations, incurring additional complexity. Another important mathematical tool to deal with CSI uncertainty is random matrix theory, where the linear precoders could be adapted to the stochastic forms according to the level of available channel knowledge. While providing a low-cost computation with reasonable performance, the drawback in this approach is that they need to be built on existing assumptions on the modeled system, e.g., the used precoding scheme, knowledge on the channel state, making their results dependent on the system specification and lacking the ability to generalize.

III. SYSTEM MODEL AND FORMULATION

A. System Model

We consider a Massive MIMO network deployed in a two-tier HetNet topology, with a macro-cell covered by MBS and small cells of SBSs on top of it, as illustrated by Fig. 1. MBS also acts
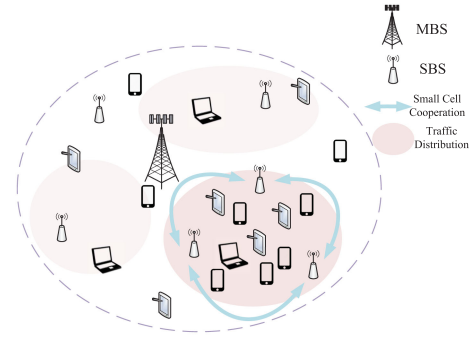

Fig. 1.   The system diagram of the scenario under consideration.

as a central controller where the inter-cell coordination takes place. There is a set of BSs $\mathcal{B} = \{0, 1, \cdots, B\}$, with MBS as the 0-th one, and the other B SBSs. Each BS $b \in \mathcal{B}$ is equipped with M antennas and associated with K users, and the sets of antennas and users are denoted $\mathcal{A}_b$ and $\mathcal{U}_b$. Note that treating the number of users per cell as uniform is done for the clarity of presentation and analysis rather than as a requirement in order to apply the proposed method. Our solution does not operate on the assumption that each cell must contain an equal amount of user equipment, and can be applied on problems with a varying number of users per cell.

The system works in a static time division duplex (TDD) manner for the up- and down-link so that the CSI estimation from the uplink transmission can be used in the downlink. During one coherence block, the channel is considered flat, and we denote the channel state between BS b to the k-th user associated with BS b' as $\mathbf{h}_{bb'k} \in \mathbb{C}^M$, drawn from a circularly-symmetric normal distribution $\mathcal{CN}(0, \mathbf{R}_{bb'k})$, where the Hermitian matrix $\mathbf{R}_{bb'k} \in \mathbb{C}^{M \times M}$ is the channel correlation characterizing the spatial correlation between the base station antennas. Unless otherwise noted, the channel correlation is generated with $\mathbf{R}_{bb'k} = \beta_{bb'k}\mathbf{I}_M$, with $\beta_{bb'k}$ modeling the large-scale fading determined mainly by environment parameters and user locations, and $\mathbf{I}$ is an identity matrix of rank M.

With linear precoding, $\mathbf{w}_{b,k} \in \mathbb{C}^K$ are the precoding vectors used by BS b intended for transmission to its own user bk. Each user receives the signal with an additive noise denoted by n_{bk}. The signal $s_{b,k} \sim \mathcal{CN}(0, 1)$ is assumed to be drawn from a Gaussian code book, and the received baseband equivalent signal of an SBS user can be expressed as

$$y_{bk} = \mathbf{h}_{bbk}^H \mathbf{w}_{bk} s_{bk} + \sum_{i \neq k, i \in \mathcal{U}_b} \mathbf{h}_{bbk}^H \mathbf{w}_{bi} s_{bi}$$
$$+ \sum_{i \in \mathcal{B} \backslash b} \mathbf{h}_{ibk}^H \sum_{j \in \mathcal{U}_i} \mathbf{w}_{ij} s_{ij} + \mathrm{n}_{bk}. \qquad (1)$$

The received signal is the sum of useful signal power, the intra-cell interference from users in the same cell, and all SBS users' signals are treated as the inter-cell interference plus receiver noise.

From the signal models, the corresponding receiver signal to interference plus noise ratio (SINR) and the achievable rate of

user k in cell b occupying bandwidth B follow:

$$\text{SINR}_{b_k} = \frac{|\mathbf{h}_{bbk}^H \mathbf{w}_{bk}|^2}{I_{bk} + N_{bk}} \tag{2a}$$

$$I_{bk} = \sum_{i \neq k, i \in \mathcal{U}_b} |\mathbf{h}_{b,bk}^H \mathbf{w}_{bi}|^2 + \sum_{i \in \mathcal{B} \backslash b} \sum_{j \in \mathcal{U}_i} |\mathbf{h}_{i,bk}^H \mathbf{w}_{ij}|^2 \tag{2b}$$

$$r_{bk} = B \log(1 + \text{SINR}_{b_k}) \tag{2c}$$

where I_{bk} is the interference power expressed as the sum of intra- and inter-cell interference, and N_{bk} is the noise power of the user across the used spectral band.

B. Power Model

The power of a Massive MIMO BS should be modeled in a way that reflects the real-world operating costs. A simplified model where the amortized power level decreases to zero as the number of antennas goes to infinity is unrealistic in EE analysis, since the diminishing return of SE and non-linear increase in system power cost are not considered. To remedy this, the BS power consumption is modeled as a sum of dynamic and static components. The dynamic power is largely due to the radio transmission activity, directly controlled by the precoding vector used. It also considers the power spent on signal processing, treated as a linear function of the achieved cell throughput [28]. It encompasses the power used to encode and decode symbols, estimate channels and calculate necessary control signals as well as the backhaul transmission costs.

The static power models the overhead for cooling and hardware basic operating power consumption. It is the sum of a constant term and a linear function of the number of active antennas, which is determined during the precoding calculation. This is to encourage the BS to use less antennas whenever possible to improve the overall energy efficiency.

In summary, the total power consumption by a base station b is:

$$P_b = \underbrace{\sum_{k \in \mathcal{U}_b} ||\mathbf{w}_{bk}||_2^2}_{\text{radio trans.}} + \underbrace{N_b P_{\text{ant}}}_{\text{antenna}} + \underbrace{\sum_{k \in \mathcal{U}} r_{bk} \cdot P_{\text{SP-Unit}}}_{\text{signal proc.}} + P_{\text{fixed}}, \tag{3}$$

where N_b is the number of *active* antennas with the constant P_{ant} the power cost per antenna; P_{fixed} is the constant term for other power consumption and r_k is the data rate for the k-th user in the current cell; $P_{\text{SP-Unit}}$ is the signal processing power per unit data flow.

C. Sparse Solution

Since the base station power constitutes almost 60% of all power usage in a communication system, and the majority of them is dedicated to radio circuits, it is necessary to try to find precoding vectors that utilize few antennas when it is feasible, e.g., when the QoS requirements are satisfied in low data-demand scenarios. Although this may contradict with the main features of Massive MIMO, whose gain results from adding BS antennas to maximize the utilization of degree-of-freedoms available in the channel, it could be beneficial to turn off the excess antennas when high throughput is less important than energy saving. In terms of optimization this could translate into a penalty term that measure the sparseness of the solutions.

The optimization problem combining constraints on sparsity has been explored, e.g. in [29]. Optimally, antennas which when put together do not improve diversity gains should not be selected. From this starting point many reported heuristics base their calculation on the channel correlation [30], or in the simple case select those with the strongest channel. However, it remains to be seen if there is a way to directly calculate a good subset of antennae for transmitting in a real-world setting, because the problem is a combinatorial programming known to be NP-hard. This class of sparse solution problems finds many uses in classification, machine learning and signal processing. One common way of approximating this problem is to use $\mathcal{L}_1$ norm, because it is equivalent to $\mathcal{L}_0$ asymptotically in the high dimension regime.

If we stack the K M-dimensional precoding vectors as $\mathbf{W}_b$, the number of active antennas N_b, as appeared in Fig. 3, is equal to the number of non-zero column vectors in the precoding matrix $\mathbf{W}_b$:

$$N_b(\mathbf{W}_b) = ||\text{diag}(\mathbf{W}_b^H \mathbf{W}_b)||_0, \tag{4}$$

where $|| \cdot ||_0$ is the number of non-zero elements in a vector and diag operation takes the diagonal elements from a matrix to form a vector. Such an addition is by no means trivial; it forces the solved solution to have group sparsity in the precoding vectors. $\mathcal{L}_0$ norms as constraints essentially transform the original problem to a combinatorial optimization — since it is reducible to solving a OPTIMUM SUBSET problem, which is of NP-hard class. Moreover, its presence is troublesome for numerical algorithms as it is not differentiable: this results in searching in a discrete space and often inefficient. In this paper, we consider a smooth transformation of the problem to enable the use of gradient-based methods.

D. Problem Formulation

With the above models, we state the problem under consideration. The goal is to maximize the SBS EE within a BS cluster $\mathcal{B}$ by choosing the optimal precoding vectors $\{\mathbf{w}_{bk}\}_{bk}$ for all b and k, given the channel states $\mathbf{h}$.

Since each BS can have its own EE, we scalarize the objective with a utility function $U : \mathbb{R}^B \mapsto \mathbb{R}$. We consider the summation of the individual EE for illustration, although as long as it is twice differentiable with a separate structure: $U(\boldsymbol{\eta}) = \sum_b U_b(\boldsymbol{\eta}_b)$ the following analysis still applies. Constraints (5b) requires that individual user rates need to be larger than a fixed lowest value $\underline{r}$, which is considered a minimum to maintain any meaningful level of service quality. Equation (5c) provides a hard limit on the total power per BS, denoted as $\bar{P}_{BS}$. Then the problem is expressed as:

$$\underset{\mathbf{w}}{\text{maximize}} \ U(\boldsymbol{\eta}) = \sum_{b \in \mathcal{B}} \eta_b = \sum_{b \in \mathcal{B}} \frac{\sum_{k \in \mathcal{U}_b} r_{bk}}{P_b} \tag{5a}$$

$$\text{s.t.} \ r_{bk} \geq \underline{r} \quad \forall b, k \tag{5b}$$

$$P_b \leq \bar{P}_{BS} \quad \forall b \tag{5c}$$

$$\text{Eqs. (2) to (4)} \quad \forall b, k, \tag{5d}$$

where the sparseness term is contained implicitly in P_b.

It may be argued that another important technique *user association* should also be used for improved efficiency, because it is likely that base stations could choose to only serve users with good enough channel conditions and therefore do not need to overly compensate for users with poor channels.

However, we find that including it typically involves knowing the channel condition between a given user and potential base stations. This is not compatible with our goal here, because we intend to use decentralized update algorithms to cut down the amount of information needed. In our current algorithm, each cell do not need to know the channel conditions between its user and out-of-cell users.

Moreover, given the settings used in the paper, the antennas and associated RF components constitute a significant portion of the power budget, and a large part of that is contributed by the *static* components. This means power savings from differently associated users is not as great as switching some of them off. Based on these concerns and limited space, in this article we consider antenna selection as a more effective component in achieving higher system energy efficiency and do not include other techniques.

IV. DECENTRALIZED PRECODING ALGORITHM

The problem in its current form cannot be solved efficiently with existing numerical techniques. The technical difficulties are two-fold, namely,

1) the objective function and the constraint functions are non-convex and involve integer variables;
2) the interference calculation requires the central controller to obtain and operate on a large scale matrix.

To deal with these issues, we transform the original problem in Eq. (5) with the following steps.

A. Auxiliary Variables for Constraints

Auxiliary variables are introduced to act as the upper and lower bounds in the original non-linear equality constraints. The purpose of this step is to eliminate the non-linear equality constraints, because even when the non-linear functions are convex, equality constraints containing them cannot be convex; hence it is necessary to put them into inequality forms; also this step reduces the amount of coupled terms between the constraints such that it is easier to analyze and solve with existing algorithmic frameworks. This is done by using the following auxiliary variables. Specifically, for all base stations indexed by b and users indexed by k, $t_b k$ is an upper bound of the interference power received by user k in cell b, ξ_{bk} and ζ_{bk} are a lower and an upper bound of user spectral efficiency; P_b is an upper bound of base station power and eta_b is a lower bound of its energy efficiency.

With Proposition 1, one can see that at optimum such inequalities will all turn to equalities. However, the constraints that come with the non-convex, non-smooth terms are still present

and needs to be treated in the algorithm development.

$$\underset{\mathbf{w}, \boldsymbol{\rho}, \hat{\mathbf{P}}, \mathbf{t}, \boldsymbol{\xi}, \boldsymbol{\zeta}, \mathbf{s}}{\text{minimize}} \quad -\sum_{b \in \mathcal{B}} \eta_b \tag{6a}$$

$$\text{s.t.} \quad \sum_{k \in \mathcal{U}_b} \xi_{bk} \geq \hat{P}_b \rho_b \quad \forall b \tag{6b}$$

$$I_{bk} + N_{bk} \leq t_{bk}, \quad \forall b, k \tag{6c}$$

$$|\mathbf{h}_{b,bk}^H \mathbf{w}_{bk}|^2 \geq s_{bk} t_{bk}, \quad \forall b, k \tag{6d}$$

$$\zeta_{bk} \geq \log_2(1 + s_{bk}) \geq \xi_{bk}, \quad \forall b, k \tag{6e}$$

$$\sum_{k \in \mathcal{U}_b} ||\mathbf{w}_{bk}||_2^2 + N_b P_{\text{ant}} + P_{\text{fixed}}$$

$$+ \sum_{k \in \mathcal{U}_b} \zeta_{bk} \cdot P_{\text{SP-Unit}} \leq \hat{P}_b \quad \forall b \tag{6f}$$

$$\hat{P}_b \leq \bar{P}_{BS} \tag{6g}$$

$$\xi_{bk} \geq \underline{r} \tag{6h}$$

Proposition 1: Problem (6) has the same optimal solution to problem (5).

Proof: If the constraints with newly added variables are equal at optimum, we can easily check that it is equivalent to any optimum of the Problem (6). Then by contradiction one can see that these constraints cannot possibly take strict inequality signs at optimum. For example, if Eq. (3) were to take strict less than, then one can choose a lower value for $\hat{P}_b$ such that equality is assumed, without violating other constraints. Moreover, with smaller $\hat{P}_b$, the lower bound ρ_b can be increased which leads to a lower objective. The same arguments can be made for all newly modified constraints, because any strict inequality would result in "free lunch", the adjustments that do not violate existing constraints and improve the objective values. Hence we can say that these constraints must be equal at optimum, at which point it is the same as the problem before the transformation. ∎

B. Approximately Optimize Antenna Activation

For optimizing the antenna selection in this manner there are methods, e.g., the typically used branch-and-bound[31]. Alternatively, one may use a greedy-based heuristic antenna selection procedure first for picking out a reasonably good subset. Here we propose to use a smoothing approximation to include antenna selection into our algorithmic framework, which incurs a lower complexity and naturally lends its form to gradient-based methods.

This method is inspired by a common approach in integer programming randomized rounding. By this approach, to solve an optimization problem with integer variables, first these integer variables are relaxed into continuous variables and a continuous solution is obtained. Then according to certain rules, the relaxed variables are turned into integers. For a certain class of problems, there are theoretical guarantees [32] on the performance of randomized rounding. In principle, what we have done is to relax the integer variables into expectations of a distribution. The distribution is designed in a way such that it leans towards
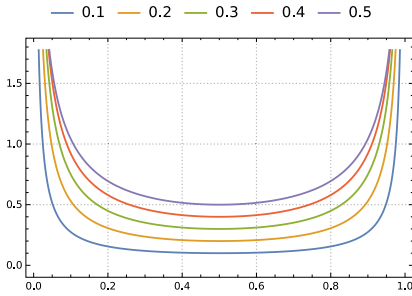
Fig. 2. The Concrete Distribution when $\alpha = 1$ and β takes different values. Notice the similarity with Bernoulli distribution when β is close to 0.

taking values close to 0 or 1, which facilitates the rounding. This approach has been used by work in other fields such as machine learning to learn a sparse model structure [33].

The key observation towards making such an approximation is to associate all antennas j in the BS b with random variables $\boldsymbol{\pi} = \{\pi_{mb}\}_{b\in\mathcal{B}, m\in\mathcal{A}_b}$, which may be called "switch variables" and take on values in [0,1]. The precoding vector for user k in BS b changes from $\mathbf{w}_{bk} = [w_{bk,1}\, w_{bk,2} \cdots w_{bk,N_b}]^T$, where elements $w_{bk,j}$ are signal weight for one antenna j for BS user bk, to $[w_{bk,1}\pi_{b1}\, w_{bk,2}\pi_{b2} \cdots w_{bk,|\mathcal{A}_b|}\pi_{b,|\mathcal{A}_b|}]^T$. Notice that switch variables ζ are set per BS antenna and is the same across the users.

We can still see that the new precoding vector expression is connected to the original problem: if the $\boldsymbol{\pi}_b$ takes value 0 with high probability for some of its antennas more than other antennas, then we can see that it means the sparse solution is to set those precoding values $w_{bk,j}$ to zero. The natural candidate is to model ζ as binomial random variables, and tweak the success probability as an optimization variable; but its discrete nature makes it hard to work with gradient methods, so instead we consider its continuous approximation *concrete distribution* [34]. This approximation is a parametric family of continuous distributions, which are crafted to allow gradients to be derived at points that correspond to its discrete counterparts, while encouraging the samples' values to be heavily distributed at 0 or 1.

The random variable associated with each base station b can be generated by the equations Eq. (7a)–(7c), controlled by parameters η_0, η_1, α and β:

$$\pi = \min(1, \max(0, \eta)) \tag{7a}$$

$$\eta \sim q\left(\frac{\eta - \eta_0}{\eta_1 - \eta_0}; \alpha, \beta\right) \tag{7b}$$

$$q(x; \alpha, \beta) = \frac{\beta\alpha x^{-\beta-1}(1-x)^{-\beta-1}}{(\alpha x^{-\beta} + (1-x)^{-\beta})^2} \tag{7c}$$

Starting from a uniform random variable from $[\eta_0, \eta_1]$, we first normalize it to $[0,1]$ as shown in Eq. (7b). Eq. (7c) is the underlying distribution model used, which is a continuous approximated version of binary Bernoulli distribution taking a number in $[0,1]$ as the input, illustrated in Fig. 2. The "shape", or how much probability is assigned to the value at two end points

is controlled by parameters α and β. This random variable is further limited by a hard sigmoid to produce values in [0,1]. By experiment we find that it is better to have the starting neighborhood $[\eta_0, \eta_1]$ larger than $[0,1]$, e.g. $[-0.2, 1.2]$.

As a result, the number of active antennas in the precoding vector is approximated by the expectation of the number of non-zero switch values, which can be calculated from the non-zero probability of the distribution given by Eq. (7b):

$$N_b \approx \mathrm{E}\left[\sum_{j\in\mathcal{A}_b} \pi_{bj}\right] = \sum_{j\in\mathcal{U}_b}(1 - Q(0; \alpha_{bj}, \beta_{bj})) \tag{8a}$$

$$Q(x; \alpha, \beta) = Q_0\left(\frac{\eta - \eta_0}{\eta_1 - \eta_0}; \alpha, \beta\right) \tag{8b}$$

$$Q_0(x; \alpha, \beta) = \exp\left(\beta(\log x - \log(1-x)) - \log\alpha\right) / $$
$$\left(\exp\left(\beta(\log x - \log(1-x)) - \log\alpha\right) + 1\right) \tag{8c}$$

where $Q(x; \alpha, \beta)$ is the CDF of random variable η in Eq.(7a).

In this way, instead of directly optimizing precoding vectors $\mathbf{w}$ for sparse solutions, the distribution parameters $\alpha_{b,j}, \beta_{b,j}$ are optimized such that the induced distribution would push switch variables to 0 or 1 by the optimization process. The price to pay is that when evaluating the gradient information of expressions involving the precoding vector, e.g., $g(\mathbf{w})$, multiple samples must be collected and their sample mean gradient is used for optimization: $\frac{1}{S}\sum_{s=1}^{S} g(\hat{\mathbf{w}} \circ \pi^{(s)})$, where S is the number of samples of π and $\pi^{(s)}$ the s-th sample of π.

C. Decentralized Decision Making

With the increasing demand of data throughput, the number of BSs in a given area increases. However, in the evaluation of inter-cell interference I_{bk}, the current problem form needs to know all the channel state information, which in total constitute $B \times B \times K \times M$ complex numbers, a highly unrealistic demand. However, by utilizing the nature of the interference, such complexity can be reduced by communicating only the interference power contributed by each BS, which does not scale quadratically with the number of base stations. It also has the added benefit of decoupling the significant portion of computation of optimal precoding vectors, by delegating these parts to individual base stations and only communicate a small amount of information at the central node.

To start, there is the assumption that each base station can estimate the channel states with the out-of-cell users. This is possible if the out-of-cell users transmit orthogonal pilot signals such that channel estimation is useful. In this way each base station is able to calculate the amount of external interference it contributes to other cells [35], [36].

We denote ι_{bk} as the estimated amount of interference power the user k in BS b receives from all other base stations: $\iota_{bk} = \sum_{b'}\sum_{k'}\mathbf{h}_{b'bk}^H\mathbf{w}_{b'k'}$. And the vector $\Psi_b \in \mathbb{R}^{BK}$ is defined such that each element $\Psi_b[i]$, where $i = 0, \cdots BK-1$ is the index

of a user in one of the B cells, is

$$\Psi_b[i] = \begin{cases} -\iota_{bk} & \text{if } bK \leq i < bK + K \\ \sum_k |\mathbf{h}_{bb\prime k\prime}^H \mathbf{w}_{bk}|^2 & \text{if } i = b\prime k\prime \text{ for some } b\prime \neq b, k\prime \end{cases} \tag{9}$$

ι_{bk} represents the local version of the information that depends on other base stations: each base station initially does not know the exact value of ι_{bk}'s, because it does not have the channel state information from other cells to the users in its cell. However, with information exchange, the ι should converge to the value which is consistent with other cell's contributed interference. So an additional equality constraint is added to the problem such that any solution found when the algorithm exits is guaranteed make it consistent:

$$\sum_b \Psi_b = 0 \tag{10}$$

This exchange and update of local information given other BSs' information at the central node is a consensus-form programming step [37]. The motivation is from this observation: the problem can be broken down into sub-problems solvable by individual BS's if there are no *coupled* constraints, where one BS requires information from other BSs. So instead of considering them together, it is possible to start individual solving with inaccurate estimates of inter BS interference, and then merge the individual solutions at the central node where other BS's information is available. In this transformation, the cross-interference power terms are treated as the consensus value.

Instead of communicating all CSI information, now each BS only transmits $(N_c - 1) \times K$ power information, which does not scale with the massive number of antennas in our problem, and is usually quite small.

V. DECENTRALIZED PRECODING ALGORITHM

With the above transformations, we have smoothed and decoupled the constraints as much as possible; all but one constraint are functions of individual BS's own state $\mathbf{l}_b$. For clarity of notation and the following analysis, we rewrite the problem variables and constraints as follows:

$$\mathcal{L}_b = \{\mathbf{l}_b | (\text{Constraints (6b)–(6h), (8) hold})\}$$
$$\mathbf{l}_b = [\mathbf{w}_b, \alpha_b, \beta_b, u_b, v_b, t_b, c_b, t_{bk}, \phi_{bk}, r_b, \Psi_b] \tag{11}$$

where $\mathcal{L}_b$ is the feasible region of all the BS-local variables. Each BS stores the state information $\mathbf{l}_b$, which will be updated in the following iterative algorithm, containing the precoding vectors, ICI, power and EE. The global states of the interference terms are put in vector ι. The shorthand of the problem is then

$$\underset{\{\mathbf{l}_b\}_b}{\text{minimize}} \quad -U(\mathbf{l}_b)$$

$$\text{s.t.} \quad h_b(\mathbf{l}_b) \leq 0 \ \forall b \tag{12a}$$

$$\sum_b A_b \mathbf{l}_b = 0 \tag{12b}$$

where h_b is a vector-valued indicator function whenever $\mathbf{l}_b \in \mathcal{L}, \forall b$, and A_b in constraint Eq. (12b) serves to extract the

components Ψ_b from l_b, and the constraint encapsulates coupled connection between the BSs in Eq. (10).

At this point it is tempting to apply the popular ADMM method like stated in [23]. However given the non-convexity of the problem, the direct application of ADMM could result in non-convergence. To remedy this issue a widely adopted approach, known as Successive Convex Approximation (SCA) as reported in [38], which adds another outer loop outside of the ADMM iterations, causing the run time complexity to be quite high. Here we propose a novel algorithm to address these challenges. It is a combination of both multiplier and quadratic programming(QP) methods, which could solve a non-convex problem to a numerical local solution at a reasonably fast converge speed and provable convergence. Note that with non-convex problems it is generally NP-hard to ensure global optimality, hence in engineering problems, solutions satisfying Karush-Khun-Tucker (KKT) conditions are considered good enough.

We assume that the problem instances are feasible and that the local optimum points indeed satisfy the KKT conditions. The additional requirement is that the system utility function $U(\cdot)$ can be written as a sum of the individual BS utility that only depends on each BS's local state information $\mathbf{l}_b$, i.d, $U(\mathbf{l}) = \sum_b U_b(\mathbf{l}_b)$. The output is the local optimal point of the original non-convex problem. During the iterations, the notations $\boldsymbol{\mu}_b$ and $\boldsymbol{\lambda}$ are used to denote the dual variables associated with the non-convex constraints and linear equality constraints, respectively. Notice that we also assume that low-level solvers for convex and quadratic programming are available to a reasonable degree of accuracy. The algorithm can be broken down into the following major phases. Note that for notation simplicity, we omit the iteration index and instead use $\mathbf{l}_b^-$ to denote the value of $\mathbf{l}_b$ from the previous iteration and $\mathbf{l}_b^+$ to denote the new, updated value of this variable.

A. Initialize

Each BS b needs to provide an initial guess of the optimal state variables $\{\mathbf{l}_b^{(0)}\}_b$, and the corresponding dual variables $\boldsymbol{\lambda}^{(0)}$. This means that an initial precoding vector and user rate and power bounds need to be generated, which can be derived from past channel observations. The algorithm uses a few other algorithmic parameters, including the scaling coefficient $\rho > 0$, the weighing positive definite matrix $\Sigma_b \in \mathbb{S}_+^{n_l}$ to allow possible base station-specific weights, and acceptable accuracy ϵ. These values are set before running the algorithms and remain constant throughout the analysis.

B. Local State Estimation

Each BS individually evaluates the sub-problem:

$$\underset{\mathbf{l}_b}{\text{minimize}} \quad -U_b(\mathbf{l}_b) + \boldsymbol{\lambda}^{-T} A_b \mathbf{l}_b + \frac{\rho}{2} ||\mathbf{l}_b - \mathbf{l}_b^-||_{\Sigma_b}^2$$

$$\text{subject to} \quad h_b(\mathbf{l}_b) \leq 0 \tag{13}$$

This is solved in a distributed manner; each BS finds out what is best for its own objective, expressed in $\mathbf{l}_b^{\text{loc}}$, given the previous

iterate solution $\mathbf{l}_b^-$. The corresponding dual variables for constraints are denoted as $\boldsymbol{\mu}_b$. This step generates a first estimate $\hat{\mathbf{l}}_b$, which together with other calculated results would be part of the new solution in the next iteration. This is similar to the ADMM algorithm, where an Augmented Lagrangian is decomposed with respect to the individual BSs.

Note that it is not required for this step to produce an exact solution, at the risk of losing the convergence guarantee of the later analysis. For performance constrained base stations, the above problem can be approximately solved.

C. Early Termination

Notice that in the previous step, only the coupled constraint in Eq. (12b) are not enforced. So if they are satisfied, then the solutions are indeed the KKT points to the original problem. As a result the termination conditions verify if the affine constraints are satisfied *and* if the individual solutions are sufficiently close to the previous solution:

$$\rho || \sum_b \mathbf{l}_b^{\text{loc}} - \mathbf{l}_b^- ||_2^2 \leq \epsilon \tag{14a}$$

$$|| \sum_b A_b \mathbf{l}_b^{\text{loc}} ||_2^2 \leq \epsilon. \tag{14b}$$

If so, the algorithm terminates and the current solution $\hat{\mathbf{l}}_b^*$ are treated as the final solutions for all base stations.

D. Negotiation

If the above conditions do not hold, this means that very likely the individual estimation of interference powers are not correct and must be modified, as represented by the violation of the affine constraints.

The process to modify the solutions can be compared to the price negotiation method used in [39]: each agent first determines a local version of bidding, then if these local versions do not agree, use prices as indicators to fix their bidding until a consensus is reached. Similarly, at central controller a quadratic programming problem is solved to find a correction value $\Delta \mathbf{l}_b$ and corresponding dual variable $\boldsymbol{\lambda}_1$:

$$\underset{\Delta \mathbf{l}, s}{\text{minimize}} \sum_b \left(\frac{1}{2} \Delta \mathbf{l}_b^T \Gamma_b \Delta \mathbf{l}_b + \nabla^T U_b \Delta \mathbf{l}_b \right) + \boldsymbol{\lambda}^{-T} \mathbf{s} + \frac{\rho_2}{2} ||\mathbf{s}||_2^2 \tag{15a}$$

$$\text{s.t.} \quad \sum_b A_b(\mathbf{l}_b + \Delta \mathbf{l}_b) = \mathbf{s} \tag{15b}$$

$$J_b \Delta \mathbf{l}_b = 0 \quad \forall b, \tag{15c}$$

where new parameter ρ_2 is a large positive constant for the regulating term, J_b is the (potentially approximate) constraint Jacobian matrix, and Γ_b is the (potentially approximate) Lagrangian function Hessian matrix, evaluated at the current individual BS states $\{\mathbf{l}_b\}_b$:

$$\Gamma_b = \nabla^2(-U_b(\mathbf{l}_b^{\text{loc}}) + \boldsymbol{\mu}_b^T h_b(\mathbf{l}_b^{\text{loc}})) \tag{16}$$

$$J_b[i] = \begin{cases} \nabla h_b(\mathbf{l}_b^{\text{loc}})[i] & \text{if } h_b(\mathbf{l}_b^{\text{loc}})[i] = 0 \\ 0 & \text{otherwise} \end{cases} \tag{17}$$

The above problem is motivated from an application of sequential quadratic programming (SQP), a common technique for solving non-convex constrained programming. It aims to find what the best change $\Delta \mathbf{l}_b$ should be for each base station, such that the LHS of the constraint Eq. (12b) is closer to zero, the system energy efficiency is low without violating any of the constraints in Eq. (12a). To find this vector, the *trust-region* trick is used: approximate the original non-linear function with its second-order expansion and optimize this quadratic function instead. This simplifies the process because second-order optimization problems with linear constraints are readily solvable by solvers like BARON. Consider the augmented Lagrangian function:

$$\mathcal{L}(\mathbf{l}, \boldsymbol{\lambda}; \rho_2) = -\sum_b U_b(\mathbf{l}_b) + \boldsymbol{\mu}_b^T h_b(\mathbf{l}_b)$$
$$+ \boldsymbol{\lambda}^T \sum_b A_b \mathbf{l}_b + \frac{\rho_2}{2} || \sum_b A_b \mathbf{l}_b ||_2^2, \tag{18}$$

where the new parameter ρ_2 is for regulating term and is assumed to be decreased in a way that does not exceed $O(||\mathbf{l} - \mathbf{l}^*||)$. Solving the following problems gives the best directions of $\Delta \mathbf{l}$ such that the change in function value is minimized while maintaining constraints:

$$\underset{\Delta \mathbf{l}}{\text{minimize}} \quad \sum_b \mathcal{L}(\mathbf{l} + \Delta \mathbf{l}, \boldsymbol{\lambda}; \rho_2)$$
$$\text{s.t.} \quad h_b(\mathbf{l}_b + \Delta \mathbf{l}_b) \leq 0 \quad \forall b \tag{19}$$

From the theory of quadratic programming, one way to solve problem (19) approximately is to solve its quadratic expansion [40]:

$$\underset{\Delta \mathbf{l}, \mathbf{s}}{\text{minimize}} \sum_b \frac{1}{2} \Delta \mathbf{l}_b^T \Gamma_b \Delta \mathbf{l}_b + \nabla_b^T \Delta \mathbf{l}_b + \boldsymbol{\lambda}^T \mathbf{s} + \frac{\rho_2}{2} ||\mathbf{s}||_2^2$$

$$\text{subject to } h_b(\mathbf{l}_b) + J_b \Delta \mathbf{l}_b \leq 0 \quad \forall b \tag{20}$$

$$\sum_b A_b(\mathbf{l}_b + \Delta \mathbf{l}_b) = \mathbf{s} \quad \forall b$$

The constant matrices Γ_b, J_b and ∇_b are the Lagrangian Hessian, constraint Jacobian and objective gradient respectively. If we allow inaccurate gradient information, the problem has the same form with the problem solved in the negotiation step.

Solving this subproblem gives a correction $\Delta \mathbf{l}_b$ to the local solutions $\mathbf{l}_b$ gained from the previous step, so that the violation of the coupling constraint is less severe. The benefits of the usage of quadratic programming are two-fold: the superior quadratic convergence helps reduce the overhead in the correction step, and the use of a second-order term enables a simpler analysis of the convergence.

Nevertheless, to avoid direct communication of channel states, each BS needs to maintain estimates of the interference level caused by others and by itself, therefore the total memory scale in this step is $O(BK^2)$, where B and K are the numbers of cells and users per cell, respectively. In our examples this is

---

Algorithm 1: Proposed EE Optimization Algorithm.

Input: Initial solution $\{l_b^{(0)}\}_b$, dual variables $\boldsymbol{\lambda}$, numerical tolerance $\epsilon > 0$, and algorithm parameters ρ, ρ_2

Output: Optimal $\{l_b^*\}_b$

initialize $\rho \geq 0$ and positive semi-definite scaling matrix $\Sigma_i \in \mathbb{S}_+^{n_x}$;

while *True* **do**

    solve problems (13) for KKT points by base stations l_b^{loc};

    Update (approximated) Hessian and gradient information Γ_b, J_b and ∇_b;

    if $|| \sum_b A_b l_b^* || \leq \epsilon$ *and* $\rho || \sum_b (\hat{l}_b - x_b)||_1 \leq \epsilon||$ **then**

        return l_b^*;

    end

    solve the coupled QP problem (15) by the central node;

    update the iterates as in Eq.(21);

end

---

still feasible because the number of cooperating cells B does not grow to a very large value, since the limiting small-cell BS hardware capabilities do not allow cooperation of a large group. Although this is an expensive step, it is amenable to standard techniques which are implemented in available solvers like SeDuMi or SNOPT. The new solution iterate is given by

$$l_b^+ = l_b + \Delta l_b$$
$$\boldsymbol{\lambda}^+ = \boldsymbol{\lambda}_1 \tag{21}$$

To further reduce the computation cost at this step, approximations can be used. In the proposed algorithm, inaccurate Jacobian update rules [40] are used to save space and time. Also Γ_b can also be the approximate version of the Hessian matrix, which can calculated with only first-order gradient information like BFGS.

The specific steps of the algorithm is listed in Algorithm 1, following the order of the previous analysis.

The proposed method can be applied to multi-antenna users by viewing a user with N_u antennas as N_u virtual single-antenna users, where each virtual users represent one single data stream. This is valid under typical application cases, when the propagation is non-line-of-sight, and there is a rich scattering environment with antennas spaced sufficiently apart. For example, an environment with many obstacles and the UEs only have a couple of antennas. In this case, the channel responses observed across the different antennas on one user are almost uncorrelated and orthogonal to each other. Therefore the multiple data streams of one user can be treated as the sum of separate "virtual users". From BS's perspective, there is no distinguishable feature to tell these virtual users apart unless the BS antennas are directional.

Likewise, the potentially different numbers of users per cell do not present a problem. It can be seen from the problem formulation as listed in Section 4, and in each constraint and objective, the difference in the per-cell user has no effect on how it is solved. Also, in the decentralization part, the messages updated between base stations are aggregates of out-of-cell influence and do not assume a specific knowledge of how many users exist.

E. Convergence Property

Assuming the final utility function is twice continuously differentiable, this algorithm then can be shown to be *locally* convergent. This means that if the estimated solution is sufficiently close to a KKT point, then the algorithm will converge to it. This is because the step in Eq. (15) follows from the convergence results of SQP methods [40].

We first show that the optimum result in the distributed optimizations of Problem (13) provide a reasonably good solution.

Lemma 1: Given twice continuously differentiable utility functions $U_b(l_b)$, and the KKT point $(l^*, \boldsymbol{\lambda}^*)$, and the condition $\nabla^2 (U_b(l_b^*) + \boldsymbol{\kappa}_b^T h_b(l_b^*)) + \rho \Sigma_i \succ 0$ holds for some $\rho > 0$ and all b, and that l and l^* are sufficiently close, then the problem (13) has locally unique minimizers $\{l_b\}_b$ such that there exist constant $k_1 > 0$, $k_2 > 0$

$$||l - l^*|| \leq k_1 ||l - l^*|| + k_2 ||\boldsymbol{\lambda} - \boldsymbol{\lambda}^*|| \tag{22}$$

Proof: From the definition,

$$l_b = \arg\min_{\hat{l}_b} L$$
$$= \arg\min_{\hat{l}_b} -U_b(\hat{l}_b) + \boldsymbol{\lambda}^T A_b \hat{l}_b + \frac{\rho}{2} ||\hat{l}_b - l_b^{(k-1)}||_{\Sigma_b}^2 \tag{23}$$

It is easy to check that the Hessian of the Lagrangian in Eq. (15a), which is

$$\nabla^2 (-U_b(l_b^*) + \boldsymbol{\kappa}_b^T h_b(l_b^*)) + \rho \Sigma_b \tag{24}$$

are all positive definite for all $(l, \boldsymbol{\lambda})$ sufficiently close to the optimum $(l^*, \boldsymbol{\lambda}^*)$. Then the minimization results in Eq. (15a) are well defined and differentiable in this neighborhood. The statement then holds because $||\frac{\partial L}{\partial x}|| < k_1$ and $||\frac{\partial L}{\partial \lambda}|| < k_2$ hold from being evaluated at KKT points. ∎

We could then show that the distance between next iterate solutions l^{k+1} and $\boldsymbol{\lambda}^{k+1}$ and the local optimal points l^* and $\boldsymbol{\lambda}^*$ diminish in a quadratic manner:

Theorem 1: (Quadratic Local Convergence) If the exact Hessian and Jacobian are used in the step Eq. (15c), then there exists a constant ρ such that

$$||l^{(k+1)} - l^*|| \leq \frac{\rho}{2} ||l^{(k)} - l^*||^2$$
$$||\boldsymbol{\lambda}^{(k+1)} - \boldsymbol{\lambda}^*|| \leq \frac{\rho}{2} ||l^{(k)} - l^*||^2 \tag{25}$$

Proof: By Theorem 11.2 from the literature [40], the update given by the quadratic program (15) is known to exhibit quadratic convergence when it follows the Newton's method update, and when the iterate point is sufficiently close to a KKT point:

$$||l^+ - l^*||_2 \leq \frac{C}{2} ||l_b - l_b^*||_2^2 \tag{26}$$

$$||\boldsymbol{\lambda}^+ - \boldsymbol{\lambda}^*|| \leq \frac{C}{2} ||l_b - l_b^*||^2 \tag{27}$$

for some constant C.

To see it is indeed a Newton's method update, one can rewrite the first order KKT condition of problem (15) in such a way,

where the update vector is left-multiplied by the gradient and the RHS is the current value:

$$\begin{bmatrix} \Gamma^* & A^T & C \\ A & \frac{1}{\rho_2}I & 0 \\ C & 0 & 0 \end{bmatrix} \begin{bmatrix} \Delta\hat{\mathbf{l}} \\ \lambda^{(k+1)} - \lambda^{(k)} \\ \kappa_{QP} \end{bmatrix} = \begin{bmatrix} \nabla_y \sum_b -U_i + A^T\lambda \\ -A\hat{\mathbf{l}} \\ 0 \end{bmatrix}$$

With exact Hessian and Jacobian matrices used here, the source of inaccuracy comes from the addition of $\frac{1}{\rho_2}I$, which goes to zero if ρ_2 is sufficiently large.

Combining this result with the above result from Lemma 1, it is not hard to arrive at

$$k_1||\mathbf{l}^{(k+1)} - \mathbf{l}^*|| + k_2||\lambda^{(k+1)} - \lambda^{(k)}||$$

$$\leq \frac{\alpha k_1 + \alpha k_2}{2}(||\mathbf{l}^{(k+1)} - \mathbf{l}^*||^2 + ||\lambda^+ - \lambda^*||^2) \quad (28)$$

given that k_1, k_2 are all positive coefficients. This establishes the local quadratic convergence. ∎

F. Additional Measure for Bad Initial Estimates

To evaluate the progress of an iterate solution, we can define the *penalty function* in terms of how severe the constraints are violated and how optimal the objective function are:

$$\mathfrak{P}(\mathbf{l}) = \sum_b -U_b(\mathbf{l}_b) + \mu_L \sum_b \mathbf{1}^T \max(h_b(\mathbf{l}_b), 0)$$

$$+ \lambda_L \sum_b ||A_b\mathbf{l}_b||_1, \quad (29)$$

where $\boldsymbol{\mu}_L$ and $\boldsymbol{\lambda}_L$ are sufficiently large positive constants. This function can only achieve the minimum value at an optimal point of the original problem. Due to the problem's non-convexity, it is possible for the algorithms to be stuck in regions where the variables change their values but $\mathfrak{P}$ stagnates due to bad initial values.

Considering this, if the difference in the penalty value between successive steps, defined as $\Delta\mathfrak{P} = \mathfrak{P}(\mathbf{l}^-) - \mathfrak{P}(\mathbf{l}^+)$, is guaranteed to be lowered bounded by a constant positive number no matter where the initial point is, then the convergence is always guaranteed. We show that such property is achievable by introducing additional steps in the variable update, thus ensuring the robustness of the proposed method. First, one can show an easily satisfied condition that ensures the algorithm convergence no matter where the initial point is.

Lemma 2: If the difference of successive penalty function is lower bounded by

$$k_3\left(\sum_b \frac{\rho}{2}||\mathbf{l}_b^{\text{loc}} - \mathbf{l}_b^-||_{\Sigma_b}^2 + \lambda_L||\sum_b A_b\mathbf{l}_b^{\text{loc}}||_1\right), \quad (30)$$

where k_3 is a very small positive constant, then the algorithm always terminates after a finite number of iterations.

Proof: We prove by contradiction. Suppose that the algorithm cannot terminate. This means that either one of the termination conditions in Eq. (14) is not met, so either one of the following is true for infinitely many iterations:

$$||\sum_b A_b\mathbf{l}_b^{\text{loc}}||_1 > \epsilon \quad (31a)$$

$$\rho||\sum_b \mathbf{l}_b^{\text{loc}} - \mathbf{l}_b||_{\Sigma_b}^2 > \epsilon \quad (31b)$$

Therefore expression (30) in either case must be at least as large as one of the two, implying the difference in penalty function is lower bounded:

$$\Delta\mathfrak{P} \geq k_3\left(\sum_b \frac{\rho}{2}||\mathbf{l}_b^{\text{loc}} - \mathbf{l}_b||_{\Sigma_b}^2 + \lambda_L \sum_b ||A_b\mathbf{l}_b^{\text{loc}}||_1\right) \quad (32)$$

$$\geq k_3 \min(\lambda_L\epsilon, \frac{1}{2\rho}\epsilon^2). \quad (33)$$

It is a positive constant that only depends on constants ϵ, λ_L and ρ. But when the original problem is feasible, the penalty function must have a finite minimum. This contradicts with the assumption that it happens for an infinite number of iterations. Therefore the presence of Eq. (30) is sufficient for algorithm convergence. ∎

To provide a backup solution iterate $\mathbf{l}^+$ which can always leave Eq. (30) satisfied, one can consider such an auxiliary problem:

$$\underset{\{\mathbf{l}_b^{\text{loc}}\}_b}{\text{minimize}} \sum_b -U_b(\mathbf{l}_b^{\text{loc}}) + \frac{\rho}{2}||\mathbf{l}_b^{\text{loc}} - \mathbf{l}_b||_{\Sigma_i}^2$$

$$\text{s.t.} \quad h_b(\mathbf{l}_b^{\text{loc}}) \leq 0 \quad \forall b \quad (34)$$

$$\sum_b A_b\mathbf{l}_b^{\text{loc}} = 0 \quad \forall b$$

This problem form comes from the regularization terms commonly used in proximal optimizations [41]. Solution $\mathbf{l}_b^{\text{loc}}$ to the problem (34) yields a next iteration that will satisfy the condition (30):

Lemma 3: The solution to the auxiliary problem (35) provides an update that will satisfy the sufficient convergence condition.

Proof: We start from the definition of the penalty function difference:

$$\mathfrak{P}(\mathbf{l}) - \mathfrak{P}(\mathbf{l}^{\text{loc}*})$$

$$= \sum_b \left(f_b(\mathbf{l}_b) + \frac{\rho}{2}||\mathbf{l}_b - \mathbf{l}_b||_{\Sigma_b}^2\right) + \lambda_L||\sum_b A_b\mathbf{l}_b||$$

$$+ \mu_L \sum_b \mathbf{1}^T \max\{0, h_b(\mathbf{l}_b)\}$$

$$- \sum_b \left(f_b(\mathbf{l}^{\text{loc}*}) + \frac{\rho}{2}||\mathbf{l}^{\text{loc}*} - \mathbf{l}_b||_{\Sigma_b}^2\right) - \lambda_L||\sum_b A_b\mathbf{l}^{\text{loc}*}||$$

$$- \mu_L \sum_b \mathbf{1}^T \max\{0, h_b(\mathbf{l}^{\text{loc}*})\}$$

$$\geq \frac{\rho}{2}\sum_b ||\mathbf{l}^{\text{loc}*} - \mathbf{l}_b||_{\Sigma_b}^2$$

$$= \frac{\rho}{2}\sum_b ||\mathbf{l}^{\text{loc}*} - \mathbf{l}_b||_{\Sigma_b}^2 + \lambda_L||\sum_b A_b\mathbf{l}^{\text{loc}*}||$$

The last step shows that the difference has a lower bound of the same form as the condition Eq. (30), hence it can ensure a strict lower penalty. ∎

Now that with this lemma we can always find an iterate solution than can converge, the natural step to take next is to

---

Algorithm 2: Solution Update for Improved Convergence.

Input: Previous iteration primal $\mathbf{l}^-$, solutions of QP
Step $\mathbf{l}^+$, $\boldsymbol{\lambda}$, k_3, λ_L
Result: Next iterate primal and dual variable
initialize $0 < \gamma \ll 1$;
$\Delta\mathfrak{P} \leftarrow \mathfrak{P}(\mathbf{l}^-) - \mathfrak{P}(\mathbf{l}^+)$;
if $\Delta\mathfrak{P} > k_3\left(\sum_b \frac{\rho}{2}||\mathbf{l}_b^{loc} - \mathbf{l}_b^-||_{\Sigma_b}^2 + \lambda_L||\sum_b A_b\mathbf{l}_b^{loc}||_1\right)$
  then
    return $\mathbf{l}_b^{loc} + \Delta\mathbf{l}_b^{loc}$, $\boldsymbol{\lambda}_1$
end
else
  Solve the dual auxiliary problem (35) for optimum
    $\boldsymbol{\lambda}_{aux}$;
    return $\mathbf{l}^-$, $\boldsymbol{\lambda}_{aux}$
end

---

see if it can be solved with its dual. In this way it could better blend in a primal-dual update framework employed in the main algorithm. Fortunately, the duality gap can be shown to be zero between the auxiliary problem and its dual. This is shown by the following lemma.

Lemma 4: The auxiliary problem's dual problem

$$\max_{\boldsymbol{\lambda}} \quad \min_{\mathbf{l}^{loc}} \sum_b f_b(\mathbf{l}_b^{loc}) + \boldsymbol{\lambda}^T A_b\mathbf{l}_b^{loc} + \frac{\rho}{2}||\mathbf{l}_b^{loc} - \mathbf{l}_b||_{\Sigma_b}^2 \quad (35a)$$

$$\text{s.t.} \quad h_b(\mathbf{l}_b^{loc}) \le 0 \quad \forall b \quad (35b)$$

has a zero duality gap.

Proof: This proof follows the outlines given by literature on proximal operator analysis in Theorem 1 of [42]. ∎

In effect, we discovered a sufficient condition on the iterate solution that will ensure the strict decrease in the penalty function, and then construct an auxiliary problem whose solution satisfies it. Additionally, this auxiliary problem has a dual problem where there is no duality gap, making it a natural choice in a primal-dual update iteration. With these additional tuning steps the algorithm can ensure the convergence even when the initial guess is far from the optimum solution. This process is another demonstration of the compromise between convergence and complexity commonly found in the algorithm design. These additional steps, depending on whether condition Eq. (30) is satisfied, are summarized in Algorithm 2.

VI. NUMERICAL RESULTS

This section illustrates the proposed algorithm's results in the scenario depicted in Fig. 1. We perform a system-level multi-cell simulation, where each cell covers a square area with side length L_{side}. Users are randomly placed inside each cell with a minimum and maximum distance from the BS expressed by L_{min} and L_{max}. The BSs are put together on a grid, and are assumed to "wrap-around", i.e., an upper most cell is a neighbor of a lower most cell, for equal treatment of edge users. We assume that they are connected through either fiber or wireless backhaul.

The channels are considered flat within the coherence block and the samples are i.i.d with distribution $\mathbf{h}_{b,bk} \sim \mathcal{CN}(0, \boldsymbol{\Theta}_{b,k})$,

TABLE I
LIST OF PARAMETERS' TYPICAL VALUES USED IN THE SIMULATION

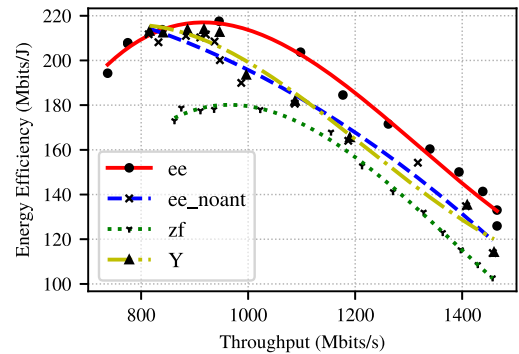| Name	Value
L_{side}	250 m
L_{min}	25 m
L_{max}	100 m
path loss α	-3.75
Shadow fading std. variance	9 dB
Gain at 1km	-147 dB
Average user power	0.1 W
Number of users per cell	10
Number of cells	4
Number of BS antennas	150
Upkeep power per antenna	0.15W
Fixed power	1W

Fig. 3. Achievable energy efficiency with system throughput.

where $\boldsymbol{\Theta}_{b,k}$ is the correlation matrix. The other experiment parameters are set in a similar fashion as in [43], [44]. We document the typical values of key parameters used in Table I.

In the simulations we consider the following approaches for comparison:
1) using the proposed algorithm with antenna selection optimization(referred to as "ee")
2) use the proposed algorithm without antenna selection optimization (referred to as "ee_noant");
3) use ADMM (hereafter denoted as "method Y") to solve for the maximum energy efficiency;
4) the most commonly used zero-forcing (ZF) precoding, with equal power distribution,

then we compare the effects of incorporating these factors to justify our choice. In Fig. 3 and Fig. 4 , the curves are fitted from the discrete dots with a polynomial.

A. Performance Evaluation

As shown in Fig. 3, we fix the number of users per cell to 10 and vary the amount of BS antennas to demonstrate the relationship of the system EE and throughput. As the number of antennas grows, there is an increase in system throughput, even when we focus on cell energy efficiency instead of throughput; this confirms the robust benefits of using more antennas for increased performance. But the system energy efficiency generally follows an inverted U-shaped trend. With more antennas, the system energy reaches a plateau quickly and then the efficiency drops.
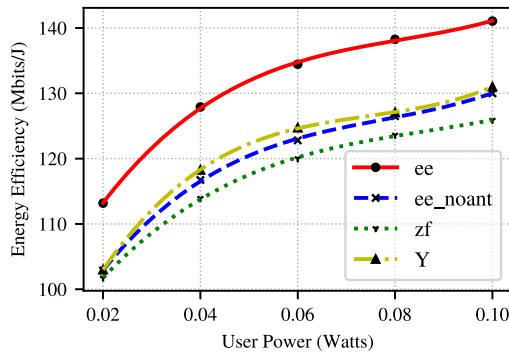
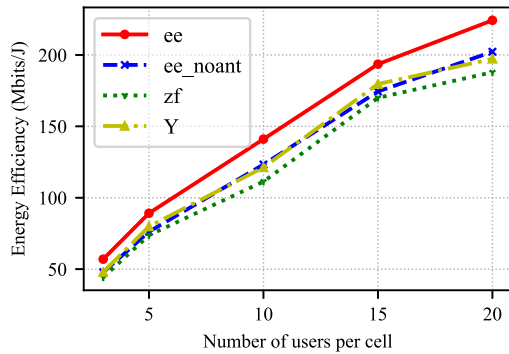Fig. 4.   Energy efficiency comparison with varying power budget.

Fig. 5.   System EE versus number of users per cell.

Fig. 6.   System EE Change versus Iterations.

Fig. 7.   System EE versus consecutive time slots.

Even when we explicitly optimize the system energy efficiency, this trend is inevitable, suggesting a potential trade-off between efficiency and throughput. The best ratio corresponding to the largest system energy efficiency as the plot shows corresponds to an antenna-user ratio between 5 to 10. Across the algorithms, the traditional zero-forcing precoding scheme proves to have good energy efficiency with simple calculations. We observe a similar level of performance between the alternate optimization algorithm, which is expected given that it optimizes the same goal. Moreover, in the high antenna number region, improved energy efficiency requires greater care in antenna selection.

In Fig. 4, we consider the effects of constraining the amount of transmission power for each user on the system energy efficiency, at a fixed system configuration that has 10 users per 120-antenna cell. These are chosen as typical values for deployment where the number of antennas is one order larger. As more power is made available, there is a steady increase in the system energy efficiency, as the system throughput increases at a faster rate than system energy cost. Again we observe that optimizing system energy efficiency results in better performance, but the benefit can be limited without turning off some antennas at the cost of lowering system throughput. The gap of performance caused by antenna selection is seen to be larger as the power increases. This can be explained by the fact that at the higher power range, it is likely to turn off some antennas to reduce a significant power cost at the cost of modest throughput loss.

Next we examine the system energy efficiency under different user numbers in a cell, as plotted in Fig. 5. We let each cell to have 110 antennas and let the number of users increase from 3 to
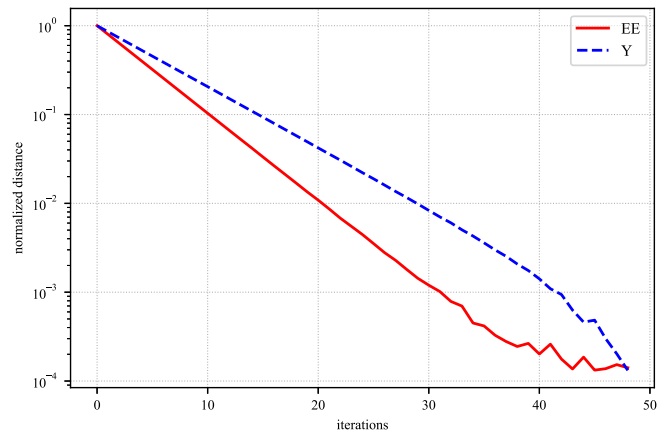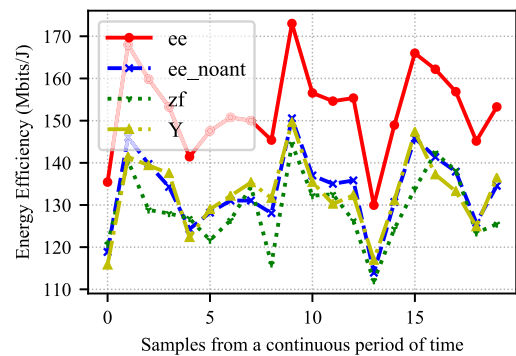
20. As expected from the theoretical performance analysis, cell energy efficiency grows almost linearly. This is because at the typical values, there is an ample degree of freedom provided by the antenna array for the optimizer to choose precoding vectors such that the interference power is very low. As the number of users grows, if the optimization goal is system efficiency, it is possible to operate at a lower throughput in exchange for less transmission power compared with ZF precoding. With additional antenna selection, larger gain can be achieved by eliminating more antenna circuit overhead from the system.

In Fig. 6, we consider the convergence performance by plotting the normalized distance between the current objective value and the optimum versus the iteration index. It is seen that in most iterations, the proposed method achieves a larger improvement. This is due to the fact that in the proposed method, each BS can independently process their parts of the channel information, and the complexity of centralized processing is significantly reduced. Even with antenna selection, the resulting convergence is faster than the alternative.

We demonstrate the achieved system EE across 20 time steps in Fig. 7. From the figure we can observe that the general trends of these methods are similar to each other, suggesting that the system EE depends heavily on the conditions of the channel realization. Also, it shows that the usage of antenna selection results in a consistent and significant system energy efficiency gain.
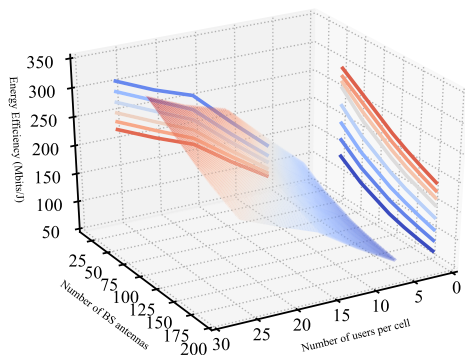
Fig. 8. System EE versus the average user count per BS and Antenna count per BS.

B. System Parameter Selection

In this subsection we are interested in using the proposed algorithm to see how it could help guide a system designer to choose appropriate parameters towards a more energy-efficient system. The scenario under consideration is a cooperating SBS cluster, and we apply the algorithm to loop through system parameters K and N_b, in the ranges $\{20-100\}$ and $\{50-200\}$ respectively, to look for the optimum system energy efficiency configurations.

We can see in Fig. 8 that even when we perform an optimum precoding scheme, the large scale system behavior remains similar to the theoretical analysis. With a growing user number per cell and a larger number of BS antennas, the energy efficiency rapidly increases to a high point, then further increase would drag the system energy efficiency down. The optimum level of BS antennas to UE closely matches the one-order-of-magnitude thumb rule, ranging from 3–8, depending on the system configurations.

The results suggest that 1) using massive MIMO BSs is the way for high energy efficiency communication system, and despite a more refined BS power modeling, its high spectral efficiency is still a dominant factor in its energy efficiency; 2) achieving high EE in massive MIMO is sensitive to many parameters like hardware efficiency and signal processing cost, hence system designers need to build a robust and representative model to fully utilize its potential; 3) EE as a design goal is in most cases not optimum in SE or power consumption; it is neither an indicator of Pareto optimality. When it comes to a multi-objective optimization problem like this, energy efficiency can only serve as an estimation of system efficiency.

VII. SUMMARY

In this paper we consider the energy-efficient control of BS power allocation, switching policy, antenna selection and beamforming in an integrated framework, in the setting of two-tier Massive MIMO HetNet. We formulate this problem as a network utility maximization problem, and propose a decentralized algorithm to solve it, using numerical techniques from sequential quadratic programming and augmented multipliers. The proposed scheme is evaluated in numerical experiments and is demonstrated to achieve a superior performance against commonly used heuristics. Our findings confirm that the optimized

system energy can be decreased with more antenna element due to the power cost, and even more users does not monotonously increase the system energy efficiency. For future research, we consider it highly promising to continue testing efficient algorithms that reduce power cost in the antenna domain, and combine it with cross-layer techniques such as user association for higher efficiency.

REFERENCES

[1] B. Mao, Y. Kawamoto, and N. Kato, "AI-based joint optimization of qos and security for 6G energy harvesting internet of things," *IEEE Internet Things J.*, vol. 7, no. 8, pp. 7032–7042, Aug. 2020.
[2] X. Cao, L. Liu, Y. Cheng, and X. Shen, "Towards energy- efficient wireless networking in the big data era: A survey," *IEEE Commun. Surv. Tut.*, vol. 20, no. 1, pp. 303–332, Nov. 2017.
[3] H. Guo, J. Liu, Z. M. Fadlullah, and N. Kato, "On minimizing energy consumption in wifi enhanced LTE-A HetNets," *IEEE Trans. Emerging Topics Comput.*, vol. 6, no. 4, pp. 579–591, Oct.–Dec. 2018.
[4] 3GPP, "Release description; release 16," 3rd Generation Partnership Project (3GPP), vol. 25, no. 996, Jul. 2018.
[5] T. L. Marzetta, "Noncooperative cellular wireless with unlimited numbers of base station antennas," *IEEE Trans. Wireless Commun.*, vol. 9, no. 11, pp. 3590–3600, Nov. 2010.
[6] N. P. Le, F. Safaei, and L. C. Tran, "Antenna selection strategies for MIMO-OFDM wireless systems: An energy efficiency perspective," *IEEE Trans. Veh. Technol.*, vol. 65, no. 4, pp. 2048–2062, Apr. 2016.
[7] L. Zhang, L. Gui, K. Ying, and Q. Qin, "Clustering based hybrid precoding design for multi-user massive MIMO systems," *IEEE Trans. Veh. Technol.*, vol. 68, no. 12, pp. 12164-12178, Dec. 2019.
[8] S. Malkowsky and Lunds universitet, *Massive MIMO: Prototyping, Proof-of-Concept and Implementation*, Doctoral thesis, Dept. Elect. Inf. Tech., Lund University, Sweden, 2019.
[9] L. Liu, B. Yin, S. Zhang, X. Cao, and Y. Cheng, "Deep learning meets wireless network optimization: Identify critical links," *IEEE Trans. Netw. Sci. and Eng.*, vol. 7, no. 1, pp. 167–180, Jan.–Mar. 2020.
[10] L. Liu, Y. Cheng, X. Cao, S. Zhou, Z. Niu, and P. Wang, "Joint optimization of scheduling and power control in wireless networks: Multi-dimensional modeling and decomposition," *IEEE Trans. Mobile Comput.*, vol. 18, no. 7, pp. 1585–1600, Jul. 2019.
[11] S. Qiu, Da Chen, D. Qu, K. Luo, and T. Jiang, "Downlink precoding with mixed statistical and imperfect instantaneous CSI for massive MIMO systems," *IEEE Trans. Veh. Technol.*, vol. 67, no. 4, pp. 3028–3041, Apr. 2018.
[12] R. Dong, A. Li, W. Hardjawana, Y. Li, X. Ge, and B. Vucetic, "Joint beamforming and user association scheme for full-dimension massive MIMO networks," *IEEE Trans. Veh. Technol.*, vol. 68, no. 8, pp. 7733–7746, Aug. 2019.
[13] G. Dong, H. Zhang, S. Jin, and D. Yuan, "Energy-efficiency- oriented joint user association and power allocation in distributed massive MIMO systems," *IEEE Trans. Veh. Technol.*, vol. 68, no. 6, pp. 5794–5808, Jun. 2019.
[14] W. Zhao, H. Nishiyama, Z. Fadlullah, N. Kato, and K. Ham- aguchi, "Dapa: Capacity optimization in wireless networks through a combined design of density of access points and partially overlapped channel allocation," *IEEE Trans. Veh. Technol.*, vol. 65, no. 5, pp. 3715–3722, May 2016.
[15] S. Rajoria, A. Trivedi, and W. W. Godfrey, "A comprehensive survey: Small cell meets massive MIMO," *Phys. Commun.*, vol. 26, pp. 40–49, Feb. 2018.
[16] C. Liu, B. Natarajan, and H. Xia, "Small cell base station sleep strategies for energy efficiency," *IEEE Trans. Veh. Technol.*, vol. 65, no. 3, pp. 1652–1661, Mar. 2016.
[17] P. Mach and Z. Becvar, "Energy-aware dynamic selection of overlay and underlay spectrum sharing for cognitive small cells," *IEEE Trans. Veh. Technol.*, vol. 66, no. 5, pp. 4120–4132, May 2017.
[18] S. Cai, Y. Che, L. Duan, J. Wang, S. Zhou, and R. Zhang, "Green 5G heterogeneous networks through dynamic smallcell operation," *IEEE J. Sel. Areas Commun.*, vol. 34, no. 5, pp. 1103–1115, May 2016.
[19] R. Razavi, L. Ho, H. Claussen, and D. Lopez-Perez, "Improving small-cell performance through switched multielement antenna systems in heterogeneous networks," *IEEE Trans. Veh. Technol.*, vol. 64, no. 7, pp. 3140–3151, Jul. 2015.

[20] M. Shariat, E. Pateromichelakis, A. U. Quddus, and R. Tafa-Zolli, "Joint TDD backhaul and access optimization in dense small-cell networks," *IEEE Trans. Veh. Technol.*, vol. 64, no. 11, pp. 5288–5299, Nov. 2015.

[21] Y. Xin, D. Wang, J. Li, H. Zhu, J. Wang, and X. You, "Area spectral efficiency and area energy efficiency of massive MIMO cellular systems," *IEEE Trans. Veh. Technol.*, vol. 65, no. 5, pp. 3243–3254, May 2016.

[22] J. Chen, "Joint antenna selection and user scheduling for massive multiuser MIMO systems with low-resolution adcs," *IEEE Trans. Veh. Technol.*, vol. 68, no. 1, pp. 1019–1024, Jan. 2019.

[23] C. Shen, T. H. Chang, K. Y. Wang, Z. Qiu, and C. Y. Chi, "Distributed robust multicell coordinated beamforming with imperfect CSI: An ADMM approach," *IEEE Trans. Signal Process.*, vol. 60, no. 6, pp. 2988–3003, Jun. 2012.

[24] J. Wang, M. Bengtsson, B. Ottersten, and D. P. Palomar, "Robust MIMO precoding for several classes of channel uncertainty," *IEEE Trans. Signal Process.*, vol. 61, no. 12, pp. 3056–3070, Jun. 2013.

[25] X. Peng, C. Ren, G. Chen, and L. Qiu, "Analysis of clustered multi-antenna small cells with intra-cluster interference cancellation," *IEEE Trans. Veh. Technol.*, vol. 68, no. 11, pp. 11343–11347, Nov. 2019.

[26] T.-H. Chang, A. Nedic, and A. Scaglione, "Distributed constrained optimization by consensus-based primal-dual perturbation method," *IEEE Trans. Autom. Control*, vol. 59, no. 6, pp. 1524–1538, Jun. 2014.

[27] Y. Shi, J. Zhang, B. O'Donoghue, and K. B. Letaief, "Large-scale convex optimization for dense wireless cooperative networks," *IEEE Trans. Signal Process.*, vol. 63, no. 18, pp. 4729–4743, Sep. 2015.

[28] F. Mahmood, E. Perrins, and L. Liu, "Energy-efficient wireless communications: From energy modeling to performance evaluation," *IEEE Trans. Veh. Technol.*, vol. 68, no. 8, pp. 7643–7654, Aug. 2019.

[29] A. Majumdar and R. K. Ward, "Fast group sparse classification," in *Proc. IEEE Pacific Rim Conf. Commun., Comput. Signal Process.*, Aug. 2009, pp. 11–16.

[30] J. Hu, Y. Cai, N. Yang, and W. Yang, "A new secure transmission scheme with outdated antenna selection," *IEEE Trans. Inform. Forensics Secur.*, vol. 10, no. 11, pp. 2435–2446, Nov. 2015.

[31] D. S. Nau, V. Kumar, and L. Kanal, "General branch and bound, and its relation to A* and AO," *Artif. Intell.*, vol. 23, no. 1, pp. 29–58, 1984.

[32] P. Raghavan and C. D. Tompson, "Randomized rounding: A technique for provably good algorithms and algorithmic proofs," *Combinatorica*, vol. 7, no. 4, pp. 365–374, Dec. 1987.

[33] C. Louizos, M. Welling, and D. P. Kingma, "Learning sparse neural networks through L_0 regularization," Jun. 2018. arXiv: 1712.01312.

[34] C. J. Maddison, A. Mnih, and Y. W. Teh, "The concrete distribution: A continuous relaxation of discrete random variables," Nov. 2016. arXiv: 1611.00712.

[35] S. Lakshminarayana, M. Assaad, and M. Debbah, "Coordinated multicell beamforming for massive MIMO: A random matrix approach," *IEEE Trans. Inf. Theory*, vol. 61, no. 6, pp. 3387–3412, Jun. 2015.

[36] G. Nauryzbayev and E. Alsusa, "Enhanced multiplexing gain using interference alignment cancellation in multi-cell MIMO networks," *IEEE Trans. Inf. Theory*, vol. 62, no. 1, pp. 357–369, Jan. 2016.

[37] A. Nedic, A. Ozdaglar, and P. A. Parrilo, "Constrained consensus and optimization in multi-agent networks," *IEEE Trans. Autom. Control*, vol. 55, no. 4, pp. 922–938, Apr. 2010.

[38] S. Zhang, L. Liu, Y. Cheng, X. Cao, and L. Cai, "Energy-efficient beamforming for massive MIMO with inter-cell interference and inaccurate CSI," in *Proc. Int. Conf. Comput., Netw. Commun.*, Mar. 2018, pp. 518–523.

[39] A. Ben-Tal and A. Nemirovski, *Lectures on Modern Convex Optimization: Analysis, Algorithms, and Engineering Applications*, Society for Industrial and Applied Mathematics, Jan. 1987.

[40] J. Nocedal and S. J. Wright, *Numerical Optimization*, 2nd ed, ser. Berlin, Germany: Springer, 2006, pp. 664.

[41] P. L. Combettes and J.-C. Pesquet, "Proximal splitting methods in signal processing," in *Fixed-Point Algorithms for Inverse Problems in Science and Engineering*, ser. Berlin, Germany: Springer, 2011, pp. 185–212.

[42] J.-J. Ruckmann and A. Shapiro, "Augmented Lagrangians in semi-infinite programming," *Math. Program.*, vol. 116, no. 1-2, pp. 499–512, Jan. 2009.

[43] D. Bethanabhotla, O. Y. Bursalioglu, H. C. Papadopoulos, and G. Caire, "User association and load balancing for cellular massive MIMO," in *Proc. Inform. Theory Appl. Workshop*, Feb. 2014, pp. 1–10.

[44] 3GPP, "Spatial channel model for multiple input multiple output (MIMO) simulations," 3rd Generation Partnership Project (3GPP), 25.996, Jul. 2018.
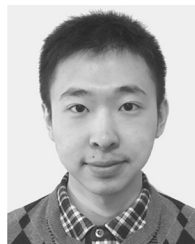
Shuai Zhang (Student Member, IEEE) received the B.Eng. and M.S. degrees from the Zhejiang University and University of California, Los Angeles, in 2013 and 2015, respectively. He is working toward the Ph.D. degree with the Illinois Institute of Technology. His research interests include wireless communication and distributed learning.
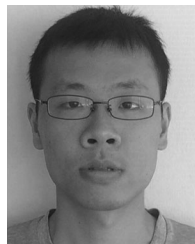
Bo Yin (Member, IEEE) received the B.E. degree in electronic information engineering and M.E. degree in electronic science and technology from Beihang University in 2010 and 2013, respectively, and received the Ph.D. degree in computer engineering from the Illinois Institute of Technology in 2020. His research interests include network security, network resource allocation, and ML-based network optimization.

Yu Cheng (Senior Member, IEEE) received the B.E. and M.E. degrees in electronic engineering from Tsinghua University in 1995 and 1998, respectively, and the Ph.D. degree in electrical and computer engineering from the University of Waterloo, Canada, in 2003. He is currently a Full Professor with the Department of Electrical and Computer Engineering, Illinois Institute of Technology. His research interests include wireless network performance analysis, information freshness, machine learning, network security, and cloud computing. He was the receipient of the Best Paper Award at QShine 2007, IEEE ICC 2011, and a Runner-Up Best Paper Award at ACM MobiHoc 2014. He was the recipient of the National Science Foundation (NSF) CAREER Award in 2011 and IIT Sigma Xi Research Award in the junior faculty division in 2013. He has served as several Symposium Co-Chairs for IEEE ICC and IEEE GLOBECOM, and Technical Program Committee (TPC) Co-Chair for IEEE/CIC ICCC 2015, ICNC 2015, and WASA 2011. He was a Founding Vice Chair of the IEEE ComSoc Technical Subcommittee on Green Communications and Computing. He was an IEEE ComSoc Distinguished Lecturer in 2016–2017. He is an Associate Editor for IEEE TRANSACTIONS ON VEHICULAR TECHNOLOGY, IEEE INTERNET OF THINGS JOURNAL, and IEEE WIRELESS COMMUNICATIONS.

Lin X. Cai (Senior Member, IEEE) received the M.A.Sc. and Ph.D. degrees in electrical and computer engineering from the University of Waterloo, Waterloo, Canada, in 2005 and 2010, respectively. She is currently an Associate Professor with the Department of Electrical and Computer Engineering, Illinois Institute of Technology, Chicago, Illinois, USA. Her research interests include green communication and networking, intelligent radio resource management, and wireless Internet of Things. She received a Post-doctoral Fellowship Award from the Natural Sciences and Engineering Research Council of Canada (NSERC) in 2010, the Best Paper Award from the IEEE Globecom 2011, the NSF Career Award in 2016, and the IIT Sigma Xi Research Award in the Junior Faculty Division in 2019. She is an Associate Editor of IEEE TRANSACTION ON WIRELESS COMMUNICATIONS, *IEEE Network Magazine*, and a Co-Chair for IEEE conferences.

Sheng Zhou (Member, IEEE) received the B.E. and Ph.D. degrees in electronic engineering from Tsinghua University, Beijing, China, in 2005 and 2011, respectively. From January to June 2010, he was a Visiting Student with the Wireless System Lab, Department of Electrical Engineering, Stanford University, Stanford, CA, USA. From November 2014 to January 2015, he was a Visiting Researcher in Central Research Lab of Hitachi Ltd., Japan. He is currently an Associate Professor with the Department of Electronic Engineering, Tsinghua University. His research interests include cross-layer design for multiple antenna systems, mobile edge computing, vehicular networks, and green wireless communications.

Hangguan Shan (Member, IEEE) received the B.Sc. degree in electrical engineering from Zhejiang University, Hangzhou, China, in 2004, and the Ph.D. degree in electrical engineering from Fudan University, Shanghai,China, in 2009. From 2009 to 2010, he was a Postdoctoral Research Fellow with the University of Waterloo, Waterloo, ON, Canada. Since 2011, he has been with the College of Information Science and Electronic Engineering, Zhejiang University, where he is currently an Associate Professor. He is also with the Zhejiang Provincial Key Laboratory of Information Processing and Communication Networks, Zhejiang University, and the Zhejiang Lab. His current research interests include cross-layer protocol design, resource allocation, and the quality-of-service provisioning in wireless networks. Dr. Shan has co-received the Best Industry Paper Award from the 2011 IEEE WCNC held in Quintana Roo, Mexico. He has served as a Technical Program Committee Member of various international conferences. He was an Editor of the IEEE TRANSACTIONS ON GREEN COMMUNICATIONS AND NETWORKING.

Zhisheng Niu (Fellow, IEEE) Graduated from Beijing Jiaotong University, China, in 1985, and received the M.E. and D.E. degrees from the Toyohashi University of Technology, Japan, in 1989 and 1992, respectively. During 1992–1994, he worked for Fujitsu Laboratories Ltd., Japan, and in 1994 joined with Tsinghua University, Beijing, China, where he is currently a Professor with the Department of Electronic Engineering. His major research interests include queueing theory, traffic engineering, mobile Internet, radio resource management of wireless networks, and green communication and networks.

Dr. Niu has been serving IEEE Communications Society since 2000 as Chair of Beijing Chapter (2000–2008), Director of Asia-Pacific Board (2008–2009), Director for Conference Publications (2010–2011), Chair of Emerging Technologies Committee (2014–2015), Director for Online Contents (2018–2019) and currently Editor-in-Chief of IEEE TRANSACTION GREEN COMMUNICATION AND NETWORKS. He was the recipient of the Best Paper Award of Asia-Pacific Board in 2013, Distinguished Technical Achievement Recognition Award of Green Communications and Computing Technical Committee in 2018, and Harold Sobol Award for Exemplary Service to Meetings and Conferences in 2019, all from IEEE Communication Society. He was selected as a Distinguished Lecturer of IEEE Communication Society (2012–2015) as well as IEEE Vehicular Technologies Society (2014–2018). He is a fellow of IEICE.